0022-1554/79/2701-0342$02.00/0
THE JOURNAL OF HISTOCHEMISTRY AND CYTOCHEMISTRY

Vol. 27, No. 1, pp. 342-349, 1979
Printed in U.S.A.

Flow Cytometry as a New Method for the Measurement of Electrophoretic Mobility of Erythrocytes Using Membrane Charge Staining by Fluoresceinated Polycations

G. VALET, S. BAMBERGER, H. HOFMANN, R. SCHINDLER, G. RUHENSTROTH-BAUER

Max-Planck-Institut für Biochemie, D-8033 Martinsried bei München, W. Germany

Received for publication July 28, 1978

The binding of FITC-labeled poly-L-ornithine and poly-L-lysine to fresh or neuraminidase treated human, rat or rabbit erythrocytes was investigated by simultaneous cell volume and cell membrane fluorescence measurements in a flow cytometer. The cell volume was converted into cell surface and the distribution curve of the fluorescence/μm^2 cell surface was calculated from all histogram classes by a computer program. The mean fluorescence/μm^2 cell surface as a measure of the density of the negative charges on the cell surface was directly proportional to the electrophoretic mobility of the erythrocytes, showing that polycation binding can effectively be used for the measurement of the electrophoretic mobility of erythrocytes. The computer fitting of the experimental two parameter histograms by two dimensional Gaussian normal distributions was found to be a very efficient way of data reduction, and a good separation of overlapping cell clusters was possible even in the case of low total numbers of cells in the histogram.

The electrophoretic mobility of cells is caused by the negative surface charges of the cell membrane. The main charge contribution comes from the carboxyl group of the *N*-acetylneuraminic acid residues covalently attached to glycoproteins (10, 13). The electrophoretic mobility is an important cell parameter because differences of the electrophoretic mobility have been used for the characterization and separation of heterogeneous cell populations in bone marrow, spleen, thymus and lymph nodes (20-23). Furthermore the electrophoretic mobility of cells may change during differentiation (23).

Several methods have been developed to determine the electrophoretic mobility of cells. Microelectrophoretic methods (2, 10, 12, 14) accurately measure the mean electrophoretic mobility of cells. It is, however, not possible to obtain reliable distribution curves of the electrophoretic mobility as they are required for the recognition of distinct cell populations because only a limited number of cells (50-100) can be measured per experiment. Electrophoresis distribution curves are obtained by analytical free flow electrophoresis (3), or laser electrophoresis (7, 15). The last two methods require cell suspensions in isotonic buffers of low ionic strength because the cell migration in buffers of physiological ionic strength is too slow. All three methods are one-parameter methods.

It would be of considerable biologic interest to measure the electrophoretic mobility of cells simultaneously with other parameters such as cell cycle phase, membrane antigens or enzymatic activities. It is also desirable to measure electrophoresis distribution curves in buffers of physiologic ionic strength in order to imitate the natural environment of cells. Flow cytometry seems suitable for such an approach, provided a charge specific fluorescence label for cell surface charges is available. We have investigated to determine if fluoresceinated polycations such as poly-L-ornithine and poly-L-lysine are useful for this purpose.

MATERIALS AND METHODS

Fluorescence labeling of polycations: Poly-L-ornithine (mean molecular weight (MMW) 122,000 daltons) and poly-L-lysine (MMW 70,000 daltons) (Sigma Chemical Co., St. Louis, Mo.) were covalently labeled with fluorescein-isothiocyanate (FITC, Merck, Darmstadt, Germany). The high M.W. polycations were chosen because the intact erythrocyte membrane is impermeable for them. The FITC concentration during labeling was 85 μg/ml *vs* 1 mg/ml of polycation at pH 9.5 in a 0.1 M NaCl, 50 mM Na_2CO_3 buffer. After 2 hr reaction at room temperature the assay was dialyzed twice for 12 hr against 1 liter of 0.95% NaCl solution buffered to pH 7.4 with 5 mM Tris/HCl (TBS). An average of one FITC residue was bound per 45 amino acid residues of the polycation under these conditions. Precipitates were formed at labeling ratios of more than one FITC residue per 30 amino acid residues.

Erythrocyte staining: Human, rat or guinea pig erythrocytes were obtained from the peripheral blood. The blood was drawn into EDTA (ethylen-diamino-tetra-acetic acid) coated polycarbonate tubes to prevent coagulation. Ten microliters of blood were washed twice with 1 ml of 0.64% NaCl solution buffered with 3 mM Tris/HCl to pH 7.4 (HTBS, 200 mOsmol) and resuspended in the same buffer at a concentration of 5×10^7 cells/ml. The erythrocytes were spheroids in the hypotonic buffer but no lysis occurred. Ten microliters of the washed human, rat or rabbit erythrocyte suspension were added to 500 μl HTBS buffer, followed by 5 μl FITC labeled polycation solution (0.5 mg/ml). The erythrocyte membrane was well and evenly stained and the cells did not aggregate or lyze. The stained erythrocytes were kept in the dark at 0°C before flow cytometric measurements.

Flow cytometric measurement: The cell volume and the cell membrane fluorescence of the stained erythrocytes were measured simultaneously in a FLUVO-Metricell flow cytometer (6). An orifice of 85 μm diameter and 100 μm length was used for the electrical size measurement with an orifice current of 0.50 mA and a particle flow between 700–1000 particles/sec. The sheath flow was HTBS buffer. The light for the fluorescence excitation was provided by a HBO-100 mercury lamp.

Data processing: The histogram data were collected and stored in a multichannel analyzer within a 64 x 64 array and transferred to magnetic tape after the end of the measurement. The histograms were plotted as three dimensional graphs and printed as isoamplitude plots (16). The stepsize in the isoamplitude plot was 10% of the maximal amplitude. According to the degree of overlap of the cell clusters in the isoamplitude plot, either analysis mode I or II was used for the calculation of the charge density distribution on the cell membrane.

Analysis I: Limiting lines for each cell cluster were drawn in the isoamplitude plot (Fig. 2) if the cell clusters were not substantially overlapping. The mean ratio of the fluorescence/μm^2 cell surface and the ratio distribution curve (Fig. 3) were calculated from all histogram classes in each area by using a computer program described earlier (16). The cell surface (S) is calculated in this program from the cell volume (V) of the spheroid erythrocytes according to the formula: $S = 4.84 \cdot (V)^{0.667}$. The mean ratio of fluorescence/μm^2 cell surface was then graphically correlated with the electrophoretic mobility (Fig. 5).

Analysis II: The analysis mode I is not accurate enough in case of widely overlapping cell clusters. We developed, in analogy to the analysis of overlapping one parameter volume distribution curves of erythrocytes (19), a FORTRAN computer program (200 kbyte core memory, Siemens 4004/150 computer) which approximates cell clusters in experimental histograms by one or several two dimensional Gaussian normal distributions. A two dimensional Gaussian distribution with the center in the origin of a (ξ, η)-coordinate system and with its axes in the ξ and η direction is defined by:

$$G(\xi, \eta) = A \cdot \exp\left(-\frac{1}{2}\left(\frac{\xi^2}{\sigma_\xi^2} + \frac{\eta^2}{\sigma_\eta^2}\right)\right) \quad [1]$$

where A = maximal amplitude of the two dimensional distribution; σ_ξ = S. D. in ξ-direction; σ_η = S. D. in η-direction. The cell clusters in experimental histograms which are to be approximated are usually shifted and rotated with respect to the origin and the axes of an (x, y)-coordinate system. A transformation of the (x, y)-coordinates into the coordinates ξ, η of an (ξ, η)-coordinate system whose origin and axes coincide with the center and the axes of the two dimensional distribution is defined by:

$$\begin{aligned} \xi &= (x - \bar{x})\cos\alpha + (y - \bar{y})\sin\alpha \\ \eta &= -(x - \bar{x})\sin\alpha + (y - \bar{y})\cos\alpha \end{aligned} \quad [2]$$

($\bar{x}$, $\bar{y}$) = coordinates of the mean value of the two dimensional distribution; α = angle of rotation between the positive x-axis and the small axis (positive ξ-axis) of the two dimensional distribution. A sum of several (N) two dimensional Gaussian distributions ($g_N(x, y)$) is defined by:

$$g_N(x, y) = \sum_{n=1}^{N} G_n(\xi_n(x, y), \eta_n(x, y))$$

where $\xi_n(x, y)$ and $\eta_n(x, y)$ is calculated with mean values ($\bar{x}_n$, $\bar{y}_n$) and rotation angles α_n according to [2], and G_n with amplitudes A_n and standard deviations $\sigma_\xi^{(n)}$ and $\sigma_\eta^{(n)}$ of the n^{th} Gaussian distribution. The input parameters for the program are estimated values for $\bar{x}$, $\bar{y}$, σ_ξ, σ_η, A and α for each two dimensional distribution. The estimated parameters of each distribution are varied by the same iterative procedure used earlier (19) until the error (E) is minimized. E is defined as the sum of squared differences

$$E = \sum_{i,j=1}^{c} (z(x_i, y_j) - g_N(x_i, y_j))^2$$

between the experimentally measured content $z(x_i, y_j)$ of the histogram classes with centers (x_i, y_j) and the sum of theoretical distributions $g_n(x_i, y_j)$ at these points. The data array was 64 histogram classes (c) in the x- as well as in the y-direction. After completion of the approximation the improved parameters are printed. Furthermore the experimental histogram, the theoretical distribution and the difference between both are plotted. The difference plot contains information if the remaining error (E) is due to a statistical scatter of the residual channel contents above or below x, y-plane (cell volume, cell fluorescence plane) or to a systematic deviation between experimental and theoretical distribution. The scatter corresponds to the statistical sampling error in the individual channels of the experimental histogram. The scatter becomes smaller with higher particle numbers in the cluster area of the histogram. For further analysis of the improved parameters it is of interest to know the S.D. σ_x and σ_y of the one parameter x and y distribution curves which are obtained by summation of each two dimensional distribution along the y or the x direction, respectively. The relation between σ_x, σ_y and the already calculated S.D. σ_ξ, σ_η is given by:

$$\sigma_x = \sqrt{\sigma_\xi^2 \cos^2\alpha + \sigma_\eta^2 \sin^2\alpha}$$

$$\sigma_y = \sqrt{\sigma_\xi^2 \sin^2\alpha + \sigma_\eta^2 \cos^2\alpha}$$

The C.V. CV_x and CV_y of the one parameter distributions are calculated as:

$$CV_x = \frac{\sigma x}{\bar{x}} 100\ (\%)$$

$$CV_y = \frac{\sigma y}{\bar{y}} 100\ (\%)$$

The mean fluorescence/μm^2 cell surface in analysis mode II is determined as ratio between $\bar{y}$ (Table I) and the cell surface which is calculated from the cell volume ($\bar{x}$, Table I) using the formula described in analysis mode I.

TABLE I

Fitting of Two Dimensional Gaussian Normal Distribution to Experimental Histograms

Erythrocytes	Mean Value (classes)		S. D. (classes)		C. V. (%)		Angle (α) of Rotation (degrees)	Contribution (%)
	$\bar{x}$	$\bar{y}$	$\sigma\xi$	$\sigma\eta$	CV_x	CV_y		
Rat	22.5	19.0	2.03	5.54	23.4	14.0	−70.4	40.4
Human	34.8	22.0	2.78	7.13	19.2	16.7	−68.6	23.7
Rabbit	29.1	14.4	1.49	4.07	13.4	12.7	−73.1	35.9

Electrophoretic mobility measurement: The mean electrophoretic mobility of erythrocytes was determined in a Zeiss microelectrophoretic system (12) in 0.95% NaCl solution buffered with 5 mM Tris/HCl to pH 7.4. The chamber was rectangular and measured 20 x 14 mm with a depth of 0.7 mm. The mean electrical field was 4 V/cm. The time for 10 μm migration of individual erythrocytes was punched on paper tape. The mean electrophoretic mobility was calculated with a digital computer from the data on the paper tapes.

Neuraminidase treatment of human erythrocytes: Human erythrocytes at a concentration of 2×10^9 cells/ml were suspended in TBS pH 7.4 containing 9 mM $CaCl_2$ and vibrio cholerae neuraminidase (Behringwerke, Marburg, Germany) at a concentration of 10 U/ml. The assay was incubated for 30 min at 37°C, washed twice with 10 ml TBS and resuspended at a concentration of 2×10^7 cells/ml in the same buffer.

RESULTS

A mixture of rabbit, human and rat erythrocytes was stained with FITC-poly-L-ornithine. The three types of erythrocytes were chosen because they differ in their electrophoretic mobilities (0.42, 1.08, 1.34 $\times$ 10^{-4} $cm^2/V \cdot sec$) and in their cell surfaces (113, 130, 98 μm^2). Both parameters are not correlated. If the flow cytometric method is valid, the fluorescence/μm^2 cell surface should indicate the surface charge density of the cell membrane irrespective of the total cell surface. The cell volume *vs* cell membrane fluoresence histogram (Fig. 1) shows two peaks (rat, rabbit) and one shoulder (human). In the isoamplitude plot (Fig. 2) the three cell clusters appear as overlapping ellipsoids. Each cluster is limited by lines for the calculations according to analysis mode I. The fluorescence/μm^2 cell surface ratios were calculated for all histogram channels and for the channels of each of the three limited areas. All ratio distribution curves were plotted (Fig. 3a, b). The ratio distribution curves of the three erythrocyte clusters are symmetrical (Fig. 3b) with C.V. of 12.8, 11.0 and 13.2% for rabbit, human and rat erythrocytes. The ratio distribution for all histogram channels (Fig. 3a) shows only two peaks. They correspond to rabbit and rat erythrocytes, while the human erythrocytes are not apparent as a separate peak or shoulder. They are hidden by the rat erythrocyte peak. The approximation of the experimental two parameter histogram (Fig. 4a) with three two-dimensional Gaussian normal distributions according to analysis mode II (Fig. 4b) is a satisfactory model because it leaves an empty cell volume-cell fluorescence plane in the difference plot (Fig. 4c). It may be argued that the human erythrocytes are not clearly visible as a separate peak (Figures 1 and 4a) or cell cluster (Fig. 2), and if this histogram was to be analyzed without knowing its composition one would not suspect the presence of a third population of erythrocytes. This is not true because approximation with two populations leaves systematic deviations from flatness in the difference plot (Fig. 4d) and C.V. in the direction of the volume axis (CV_x) is then 31%. This is not reasonable from a biological point of view because CV_x over 25% do not occur in homogeneous erythrocyte populations. Both observations are, therefore, indicators for more than two populations of cells in this histogram. The experimental histogram (Fig. 4a) contains

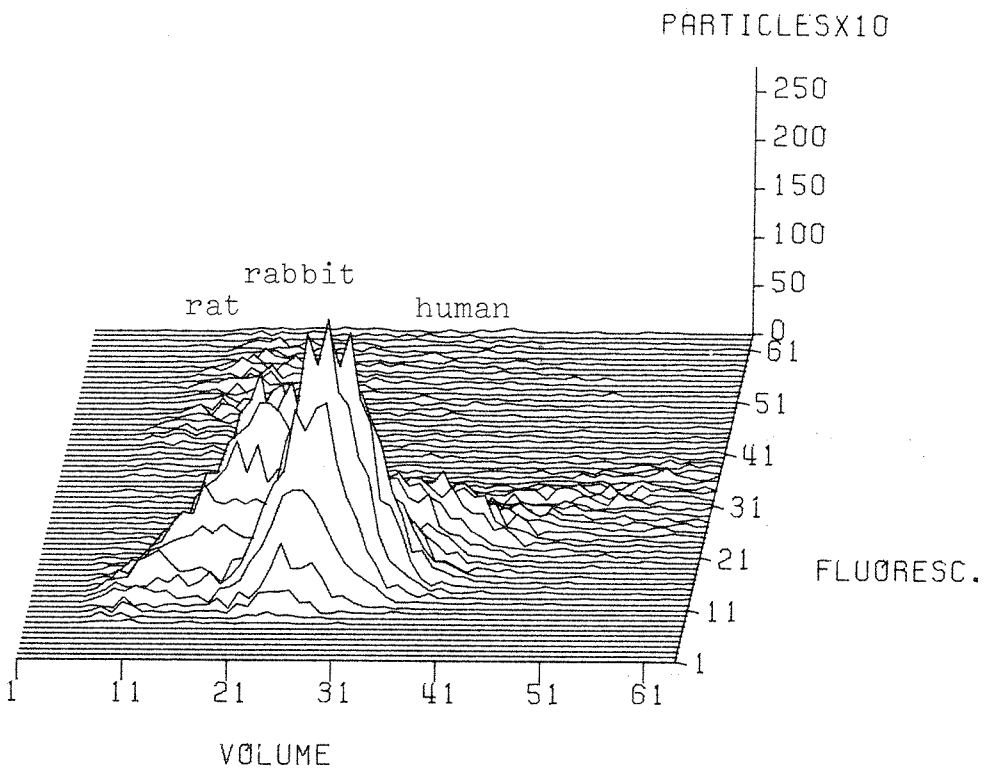

FIG. 1. Three dimensional plot of a cell volume (*x*-axis) *vs* cell fluorescence (*y*-axis) histogram of a FITC-poly-L-ornithine stained mixture of 41% rat, 35% rabbit and 24% human erythrocytes. The number of cells in each histogram class is plotted in direction of the *z*-axis. The histogram contains 34542 particles with 282 particles at the maximum amplitude.

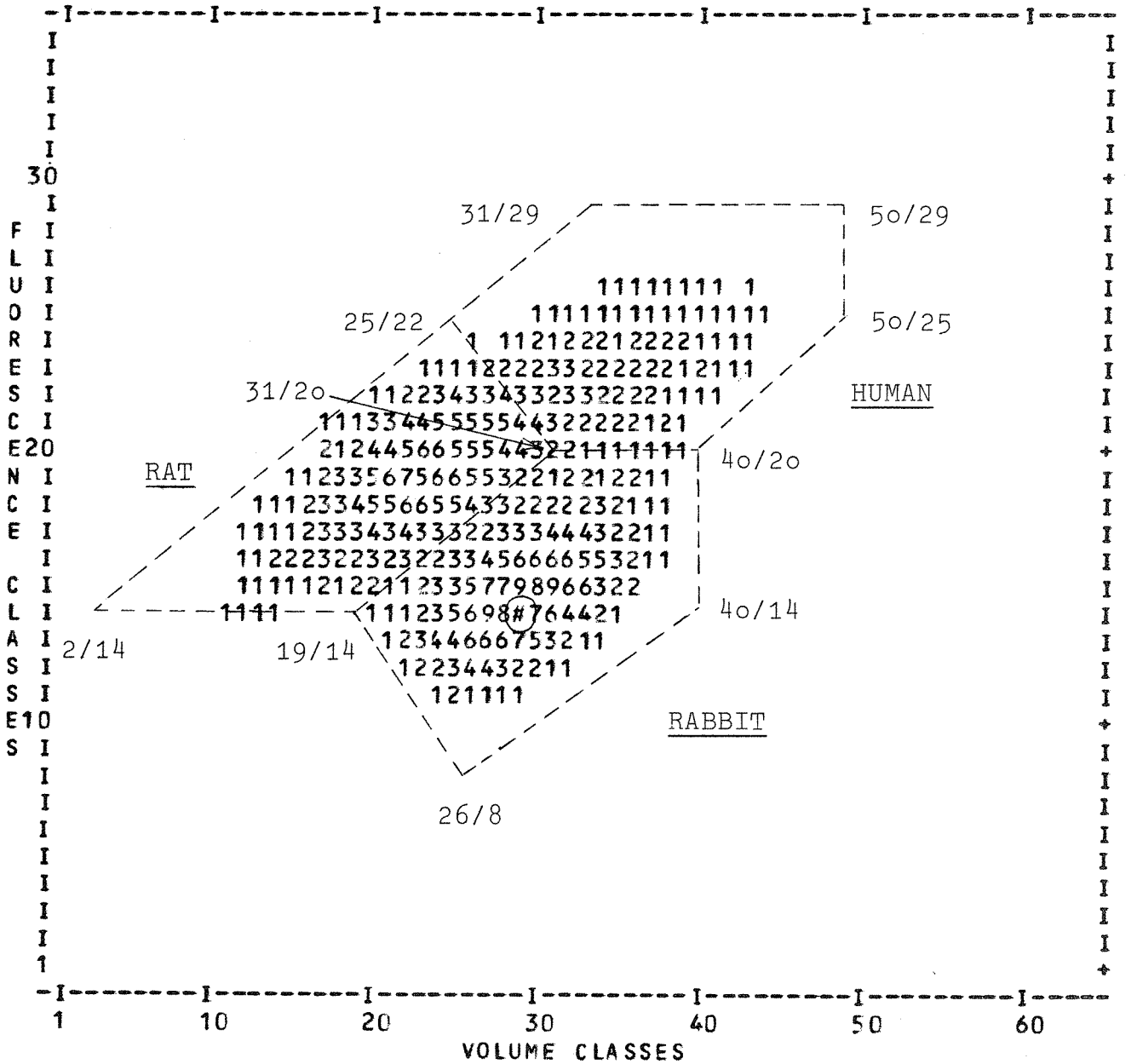

FIG. 2. Isoamplitude plot of the histogram of Figure 1 in the direction of the z-axis. The plot is normalized to the maximum amplitude ( )as 100%. The range 0–100% is divided into classes with 10% class width which are numbered from 0–9. Histogram classes with number 0 (0–9.99% of maximum) are suppressed in the printout. The broken lines limit three areas. The coordinate pairs at the corners of the areas were used for the calculation of the charge density distribution according to analysis mode. I. One volume class corresponds to 4.02 μm^3.

only 34,542 cells and 282 cells as the maximum channel content. Nevertheless this histogram was chosen as an example for the fitting of two dimensional Gaussian distributions to experimental histograms because it shows that the statistical uncertainty of the channel contents does not influence the approximation. The statistical scatter of the channel contents is left over in the difference plot (Fig. 4c) as noise above and below the cell volume-cell fluorescence plane. The advantages of the fitting of two dimensional Gaussian normal distributions are: resolution of superimposed cell clusters and efficient data reduction to a few parameters (Table I). The reduction is from $64 \times 64 = 4096$ values to 6 descriptors (factor 683) per two dimensional distribution (x_o, y_o, σ_ξ, σ_η, α, and % contribution). The reduction is much better than in a one dimensional analysis e.g. of a volume distribution curve where a 64 channel histogram is reduced to 3 descriptors (factor 21) per one dimensional Gaussian distribution (x_o, σ_x, and % contribution). The mean fluorescence/μm^2 cell surface determined by both analysis modes was plotted against the electrophoretic mobility of the erythrocytes (Fig. 5) which was determined separately by microelectrophoresis. The fluorescence/μm^2 cell surface ratios of all cell types are well corre-

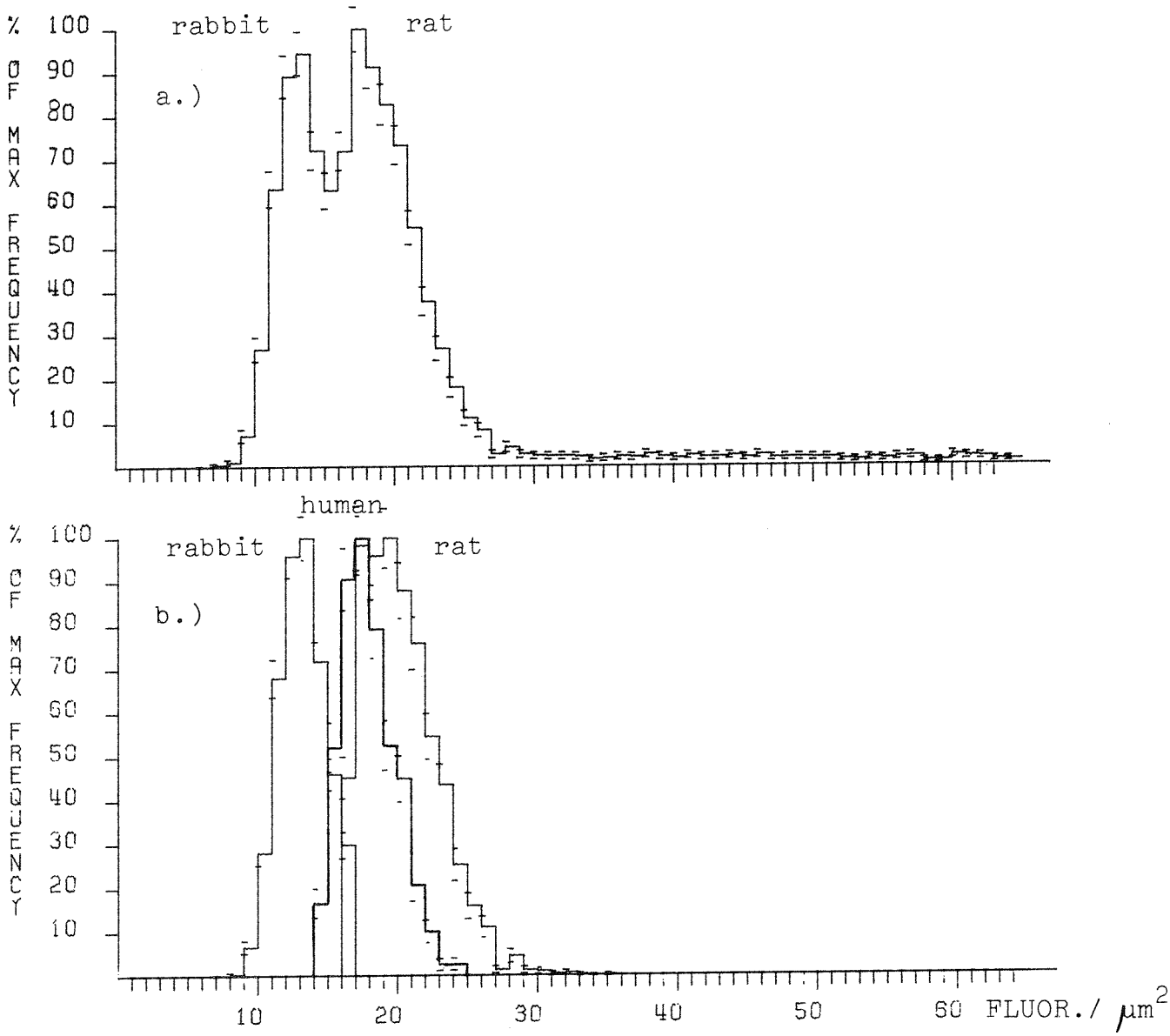

FIG. 3. Charge density distribution curve of rabbit, human and rat erythrocytes calculated according to analysis mode I from the total histogram (a) or from each cell cluster (b) of the histogram of Figure 2 separately.

lated with the electrophoretic mobility in a linear relationship. A further test for the charge specificity of polycation binding was the removal of the neuraminic acid residues from the cell membrane by incubation of human erythrocytes with neuraminidase. The decreased neuraminic acid content of the erythrocyte membrane after the incubation decreases both the polycation binding capacity of the erythrocyte membrane and the electrophoretic mobility of human erythrocytes (Fig. 5), indicating that polycation binding to erythrocyte membranes is a charge specific reaction which is adequately measured by flow cytometry. Similar results were obtained with FITC-poly-L-lysine instead of FITC-poly-L-ornithine.

DISCUSSION

The main result of this study is that binding of FITC labeled poly-L-ornithine and poly-L-lysine is proportional to the electrophoretic mobility of erythrocytes (Fig. 5). This shows that the polycations bind preferentially to those charges of the erythrocyte membrane which contribute to the electrophoretic mobility. Negative charges which are located deeper in the cell surface coat are apparently not stained. Poly-L-lysine binding has been shown to be charge specific by previous biochemical studies (1, 11). It binds preferentially to erythrocyte membrane glycoproteins. The poly-L-lysine binding of these proteins is substantially reduced or abolished if their neuraminic acid is removed (1). Poly-L-ornithine or poly-L-lysine have a strong tendency to aggregate erythrocytes (8). Aggregation does, however, not occur under our assay conditions (Fig. 4a). This is probably due to the low erythrocyte concentration (3×10^6/ml) and to the polycation concentration of 5 μg/ml. The electrophoretic mobility of human erythrocytes at this concentration is $+0.70 \times 10^{-4}$ cm^2/V·sec, as

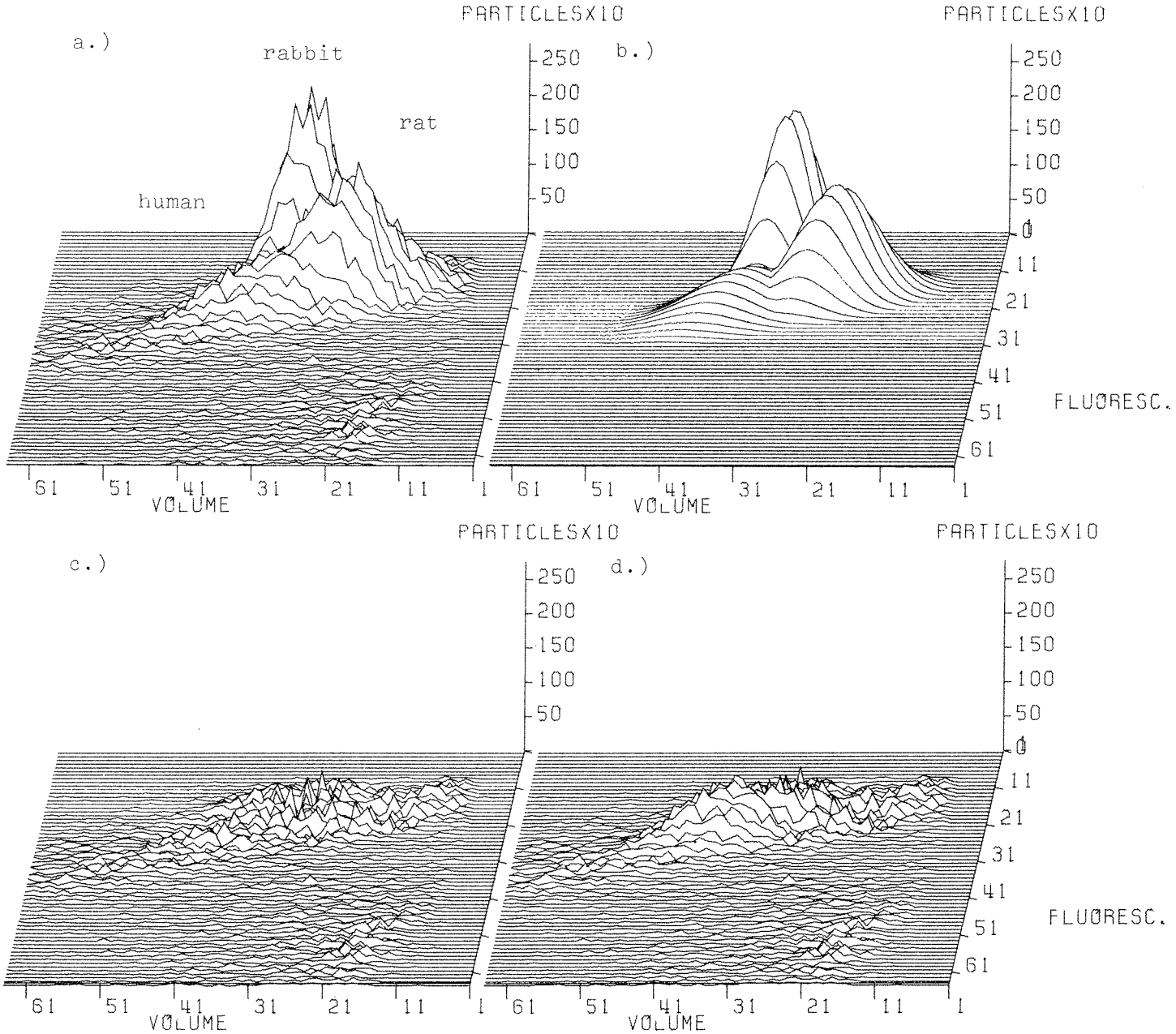

FIG. 4. Approximation of the histogram of Figure 2 (a) by three two-dimensional Gaussian normal distributions (b) according to analysis mode II. Each theoretical distribution is plotted to the point from which the next distribution has a higher amplitude. Figure 4b is therefore no additive curve. The advantage of this type of plotting is that the location of the individual theoretical distributions is better visible. The difference plot (c) between the experimental histogram and the sum of the theoretical distributions leaves an essentially flat cell volume-cell fluorescence plane. The difference plot (d) shows systematical deviations from a flat cell volume-cell fluorescence plane when the histogram is approximated by only two Gaussian distributions.

compared to zero at 2 μg/ml and -1.08×10^{-4} cm^2/V·sec without poly-L-ornithine. Similar results were obtained with poly-L-lysine. The spheroid shape of the erythrocytes in hypotonic solution is also in favor of nonaggregation because the areas of interaction are smaller in spheroid than in biconcave erythrocytes. The main purpose of erythrocyte swelling was to apply an easy formula for conversion of erythrocyte volume into erythrocyte surface. Swelling is, however, not a mandatory condition for the method because erythrocytes in isotonic solution can also be measured. Biconcave erythrocytes are deformed by the hydrodynamic acceleration forces to rotational ellipsoids in the sizing orifice (4). It is possible to calculate the surface of rotational ellipsoids if the volume and the length to diameter ratio of the ellipsoids is known. The ratio can be determined from photographs of the erythrocytes during passage through the orifice (5). This procedure is, however, more complicated than preswelling of the erythrocytes.

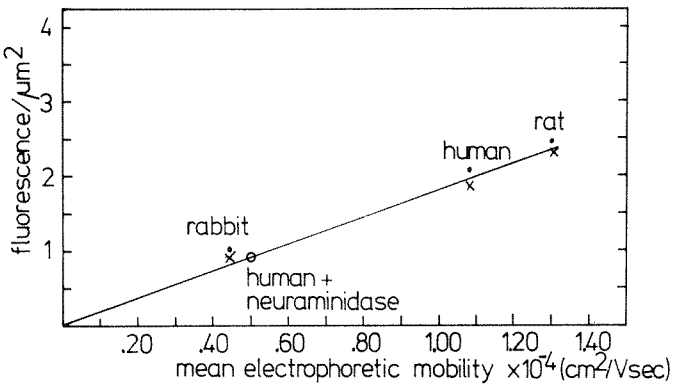

FIG. 5. Correlation between the mean electrophoretic mobility of different kinds of erythrocytes and the mean fluorescence/μm^2 cell surface after staining of the erythrocytes with FITC-poly-L-ornithine. Processing of the data according to analysis mode I (•) and analysis mode II (×) gave similar results. The fluorescence on the ordinate scale represents the number of fluorescence channels $\times 10^{-2}/\mu m^2$ cell surface.

The coefficients of variation of the flow cytometrically determined charge density distributions (Fig. 3b) are usually between 10–15%. This is comparable to the results of laser electrophoresis (15) but higher than the 3–4% C.V. obtained by the analytical free flow system (3). It should be possible to reduce the C.V. of the flow cytometric curves in the future by using higher light intensities for fluorescence excitation and smaller orifices for electrical sizing. The high C.V. decrease the resolution of distinct erythrocyte populations in the charge density distribution calculated for all erythrocytes (Fig. 3a) of the two parameter histogram (Fig. 4a). It is not possible to distinguish a separate peak or shoulder for human erythrocytes. The human erythrocyte cell cluster is, however, distinguishable in the original two parameter histogram (Fig. 2). The conclusion from this is that the resolution of the flow cytometric method is similar to the analytical free flow electrophoresis (3) provided the charge density distribution for each cell cluster is calculated separately from the two parameter histogram (Fig. 3b). The calculated charge density distribution for all erythrocytes (Fig. 3a), in contrast, is not well suited to resolve complex cell mixtures at present.

The sensitivity of the flow cytometric method is superior to all three other methods because only $0.3\text{-}1 \times 10^5$ cells are needed per measurement. This is substantially lower than the $5 \times 10^5\text{-}1 \times 10^7$ cells which are necessary in free flow, laser or microelectrophoretic systems. The low number of cells needed for the flow cytometric method is especially an advantage in cell separation studies where the number of available cells is usually limited.

An application of the flow cytometric method is the measurement of the erythrocytes of young rats, guinea pigs and sheep during the first month after birth. The mean electrophoretic mobility of the erythrocytes increases slowly during this time. Several distinct erythrocyte populations are produced by the hematopoietic tissues (17–19) within the same time period. It is of interest for the understanding of the underlying regulatory mechanisms of differentiation, whether each erythrocyte population has a different electrophoretic mobility or whether all erythrocytes gradually change their electrophoretic mobility i.e. their membrane charge architecture. Another important problem is the measurement of nucleated haematopoietic cells. The cell surface coat of these cells is thicker than that of erythrocyte membranes (22) and contains more negative charges. Their electrophoretic mobility is, however, lower than the electrophoretic mobility of erythrocytes. This means that only a fraction of all negative membrane charges contributes to the electrophoretic mobility. It is desirable to develop stains which either indicate all negative membrane charges or only those which are effective for the electrophoretic mobility.

The determination of charge density distributions on erythrocyte membranes was only possible because a combined cell volume-cell fluorescence measurement was made. It is important to realize that this type of measurement has a much broader application. It is possible to express many flow cytometric data in terms of concentration or of mean surface density if cell content signals (e.g. protein, enzyme activities, metabolites, antigens and receptors) and the cell volume are measured together. The comparison of concentration values is often more informative in a biochemical sense than a comparison of the contents of different cell types. The usefulness of the cell volume parameter in multiparameter flow cytometric measurements is therefore twofold. Volume distribution curves of cells contain information by themselves and additionally serve as reference parameter for **flow cytometric biochemistry**. One may object that in case of a preferential location of substances on certain parts of the cell membrane (caps) or within organelles (nucleus, mitochondria, Golgi apparatus) of the cytoplasm an accurate determination of the true surface densities or concentrations of substances at these locations may not be possible. This is true but compared to cell disruption, followed by biochemical measurements in homogenates or fractionated homogenates as an alternative, the flow cytometric measurement can often be performed in living cells which is an important advantage. Imaging in flow (4, 9) will become a valuable tool in the future to decide quickly whether the surface density of the cytoplasmic concentration of labeled substances in cells is homogeneously distributed or not.

LITERATURE CITED

1. Danon D, Howe C, Lee LT: Interaction of polylysine with soluble components of human erythrocytes. Biochim Biophys Acta 101: 201, 1965
2. Goetz PHJ, Penniman JG: A new technique for microelectrophoretic measurements. Am Lab October 1976
3. Hannig K, Wirth H, Schindler RK, Spiegel K: Free flow electrophoresis III. An analytical version for a rapid, quantitative determination of electrophoretic parameters. Hoppe-Seyler's Zschr. Physiol. Chem. 358:753, 1977
4. Kachel V: Basic principles of electrical sizing of cells and particles and their realization in the new instrument "Metricell". J Histochem Cytochem 24:211, 1976
5. Kachel V, Benker G, Lichtnau K, Valet G, Glossner E: Fast imaging in flow: A means of combining flow cytometry and image analysis. J Histochem Cytochem submitted
6. Kachel V, Glossner E, Kordwig E, Ruhenstroth-Bauer G: Fluvo-Metricell, a combined cell volume and cell fluorescence analyzer. J Histochem Cytochem 25:804, 1977
7. Kaplan JH, Uzgiris EE: Identification of T and B cell subpopu-

lations in human peripheral blood: Electrophoretic mobility distributions associated with surface marker characteristics. J Immol. 117:1732, 1976
8. Katchalski A, Danon D, Nevo A, DeVries A: Interactions of basic polyelectrolytes with the red blood cell. II. Agglutination of red blood cells by polymeric bases. Biochim Biophys Acta 33:120, 1959
9. Kay DB, Wheeles LI: Laser stroboscopic photography. Technique for cell orientation studies in flow. J Histochem Cytochem 24:265, 1976
10. Mehrishi JN: Molecular aspects of the mammalian cell surface. Progr Biophys Mol Biol 25:1, 1972
11. Nevo A, DeVries A, Katchalski A: Interaction of basic polyamino acids with the red blood cell. I. Combination of polylysine with single cells. Biochim Biophys Acta 17:536, 1955
12. Ruhenstroth-Bauer G, Fuhrmann GF: Cell electrophoresis employing a rectangular measuring cuvette. Cell Electrophoresis. Edited by EJ Ambrose. Churchill, London 1965, p. 22–25
13. Seaman VF: Electrokinetic behavior of red cells. The Red Blood Cell, Vol. II Edited by DMN Surgenor. Academic Press, New York 1975, p. 1135–1229
14. Seaman GVF: Electrophoresis using a cylindrical chamber. Cell electrophoresis. Edited by EJ Ambrose. JA Churchill, London 1965, p 4–21
15. Uzgiris EE, Kaplan JH: Laser doppler spectroscopic studies of the electrokinetic properties of human blood cells in dilute salt solutions. J Coll Interf Sci 55:148, 1976
16. Valet G, Hanser G, Ruhenstroth-Bauer G: Computer analysis of two parameter histograms of rat bone marrow cells. Cell volume to DNA relationship measured by means of flow cytometry. Pulse Cytophotometry III, European Press Medikon, Gent 1978, p 127–136
17. Valet G, Franz G, Lauf PK: Different red cell populations in newborn, genetically low potassium sheep: Relation to haematopoietic immunologic and physiologic differentiation. J Cell Physiol 94:215, 1978
18. Valet G, Hanser G, Ruhenstroth-Bauer G: Ein neues Konzept der Haematopoese im Säugetierorganismus während der Nachgeburts-phase: Nachweiss mehrerer Volumenpopulationen der Erythrozyten bei Ratten, Mäusen, Meerschweinchen, Kaninchen, Schafen und Ziegen. Blut 34:413, 1977
19. Valet G, Hofmann H, Ruhenstroth-Bauer G: The computer analysis of volume distribution curves. Demonstration of two erythrocyte populations of different size in the young guinea pig and analysis of the mechanism of immune lysis of cells by antibody and complement. J. Histochem. Cytochem. 24:231, 1976
20. Zeiller K, Hansen E: Characterization of rat bone marrow lymphoid cells. I. A Study of the distribution parameters of sedimentation, velocity, volume and electrophoretic mobility. J Histochem Cytochem 26:369, 1978
21. Zeiller K, Pascher G, Hannig K: B lymphocyte subpopulations in the mouse spleen. A study of the differentiation pathway using free flow electrophoretically separated subpopulations of direct PFC progenitor cells. Immunology 31:863, 1976
22. Zeiller K, Schindler R, Liebich HG: The T lymphocyte surface in development. A study of the electrokinetic, antigenic and ultrastructural properties of T lymphocytes in mouse thymus and lymph nodes. Isr J Med Sci 11:1242, 1975
23. Zeiller K, Pascher G, Wagner G, Liebich HG, Holzberg E, Hannig K: Distinct subpopulations of thymus-dependent lymphocytes. Tracing of differentiation pathways of T cells by use of preparatively electrophoretically separated mouse lymphocytes. Immunology 24:995, 1974